Classification and analysis of lateral torque-vectoring differentials using velocity diagrams

K Sawase[1*] and **K Inoue**[2]
[1]Drivetrain Engineering Department, Mitsubishi Motors Corporation, Okazaki, Japan
[2]Department of Mechanical System and Design, Tohoku University, Sendai, Japan

The manuscript was received on 31 January 2008 and was accepted after revision for publication on 19 May 2008.

DOI: 10.1243/09544070JAUTO824

Abstract: This paper describes the classification and analysis of lateral torque-vectoring differentials using velocity diagrams, which are frequently used for the gear-shifting analysis of an automatic transmission. A lateral torque-vectoring differential is composed of the mechanism of torque vectoring from the right wheel to the left wheel, and the similar mechanism of torque vectoring from the left to the right. The analysis shows that, when only the mechanism part of one-way torque vectoring is considered, then the smallest number of the rotational elements composing the one-way torque-vectoring mechanism is four. This is the simplest mechanism. The mechanism is classified into seven kinds of mechanism, namely six clutch-type mechanisms and one brake-type mechanism. The expressions for the clutch torque for torque vectoring, the clutch slip speed, and the energy loss generated by clutch are presented for these mechanisms. As a result, the theoretical value of energy loss is completely the same in these seven kinds of mechanism in the ideal state, in which the transmission efficiency of gears, agitation loss, etc., are assumed to be neglected. Finally, from an actual mechanism design point of view, the best mechanism is evaluated.

Keywords: torque vectoring, velocity diagram, driveline system, direct yaw control

1 INTRODUCTION

The direct yaw control technology was proposed in the early 1990s. For example, Shibahata *et al.* [**1**] showed that direct yaw moment control by proper distribution of traction and braking force on the right and left wheels could improve vehicle manoeuvrability. Motoyama *et al.* [**2**] made an experimental vehicle that can control traction force distribution to each of the four wheels and demonstrated the effect of lateral traction force distribution.

In particular, the direct yaw control system utilizing lateral braking force difference is very effective in stabilizing a vehicle in a critical cornering situation [**3**], so that this system has progressed and become common as the 'stability control system' since the first application was introduced with the Mercedes S series [**4**].

However, because the decrease in the vehicle speed and the large energy loss caused by braking, this system is only suitable for improving vehicle driving stability during deceleration cornering or a critical cornering situation. Meanwhile a lateral traction force distribution system can control the yaw moment with small energy loss. However, the drive torque supplied from the engine restricts its yaw moment, and so this system is only effective during acceleration cornering. Thus, both the brake yaw control system and the lateral traction force distribution control system can be used in limited driving situations.

In order to improve vehicle driving stability from the usual driving condition to the critical driving condition during a vehicle acceleration, steady state, and deceleration situation, and to provide driving pleasure to a driver, Ikushima and Sawase [**5**] proposed on other concept for generating a direct yaw moment. This concept utilizes a torque transfer

Corresponding author: Drivetrain Engineering Department, Mitsubishi Motors Corporation, 1 Nakashinkiri, Hashime-cho, Okazaki, 444-8501, Japan. email: kaoru.sawase@mitsubishi-motors.comemail: kaoru.sawase@nifty.ne.jp

mechanism between right and left wheels and generates a couple. This mechanism concept is called the 'torque-vectoring differential' (TVD).

Sawase and Sano [**6**] developed a direct yaw control system utilizing the lateral TVD and applied it to production vehicles for the first time in the world. The TVD generates the yaw moment by torque vectoring between right and left wheels without influence on vehicle acceleration or deceleration, and so the TVD can improve the vehicle dynamics limit of vehicles of various drivetrain types in any driving situation, namely acceleration, steady state, and deceleration [**7**]. In recent years, control ability comparisons of vehicle dynamics systems including the TVD, and integrated vehicle dynamics control methods with TVD have been reported [**8–10**], in which the TVD attains a high valuation.

Furthermore, various mechanisms are proposed. Among these, some electric-powered TVDs have been proposed [**11**], but this is only suitable for hybrid vehicles. Most TVDs consist of a clutch or brake for torque vectoring from the right to the left, a clutch or brake for torque vectoring from the left to the right, differential gears, and some planetary gears [**12–16**]. Because of its complicated structure, the operation and characteristics of these mechanisms are difficult to understand.

Therefore, the present authors tried to represent the characteristics of TVD by applying the velocity diagram [**17**], which is frequently used for the gear-shifting characteristic analysis of an automatic transmission [**18**]. First, this paper describes the velocity diagram analysis of the world's first production TVD, namely an active yaw control (AYC) differential. Second, all TVDs, which utilize a clutch or a brake, and which consist of minimum number of rotational elements, are examined and classified using the velocity diagram. Finally, the advantages and disadvantages of each TVD are studied.

2 DEFINITION OF LATERAL TORQUE-VECTORING DIFFERENTIAL

Figure 1 shows the definition of the lateral TVD in this paper. The TVD adjusts both the direction and the amount of vectoring torque T_V that is transmitted and received between right and left, so that it makes the driving force T_V/R_t act on one wheel and the braking force $-T_V/R_t$ act on the other side, where R_t is the dynamic tyre radius. The difference between the R_t values of the right and left tyres as well as their variation while vehicle cornering is neglected in this paper. When $T_V = 0$, the TVD distributes the drive torque T_e supplied from the engine equally to the wheels on both sides. From these definitions, the driving force D_r of the right wheel, the driving force D_l of the left wheel, the driving force difference ΔD, and the yaw moment M_g acting on the vehicle are represented as

$$D_r = \frac{T_e/2 + T_V}{R_t} \tag{1}$$

$$D_l = \frac{T_e/2 - T_V}{R_t} \tag{2}$$

$$\Delta D = D_r - D_l = \frac{2T_V}{R_t} \tag{3}$$

$$M_g = \frac{T_V}{R_t} W \tag{4}$$

where W is a vehicle track. Consequently, the TVD generates the driving force difference between right and left wheels and can control the yaw moment M_g, even if the drive torque $T_e = 0$.

In order to realize these functions, the TVD needs to have the differential gears and the torque-vectoring mechanism between right and left wheels.

It should be noted that the mechanisms reported in references [**19**] and [**20**] cannot generate the yaw moment when the drive torque $T_e = 0$; therefore these do not meet the definition of TVD. Regarding the electric-powered TVD, its application is limited to hybrid vehicles. Therefore, this paper deals with a TVD utilizing a clutch or brake.

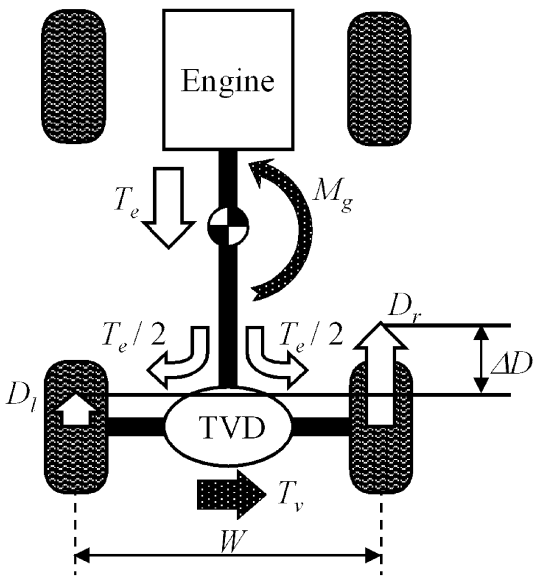

Fig. 1 Lateral TVD

3 REPRESENTATION OF TORQUE-VECTORING DIFFERENTIAL BY VELOCITY DIAGRAM

3.1 Velocity diagram of planetary gears

The simple planetary gears shown in Fig. 2(a) consist of three rotational elements, namely sun gear (SG), carrier (CA), and ring gear (RG). This is the mechanism of three elements with two degrees of freedom; therefore, when the revolution speeds of two elements are given, the revolution speed of the remaining element can be obtained. Figure 2(b) shows the velocity diagram of the simple planetary gears. The revolution speeds of three elements are indicated by the three points in the diagram, where the horizontal axis shows the ratio of revolution speeds of each element to the carrier speed used as reference.

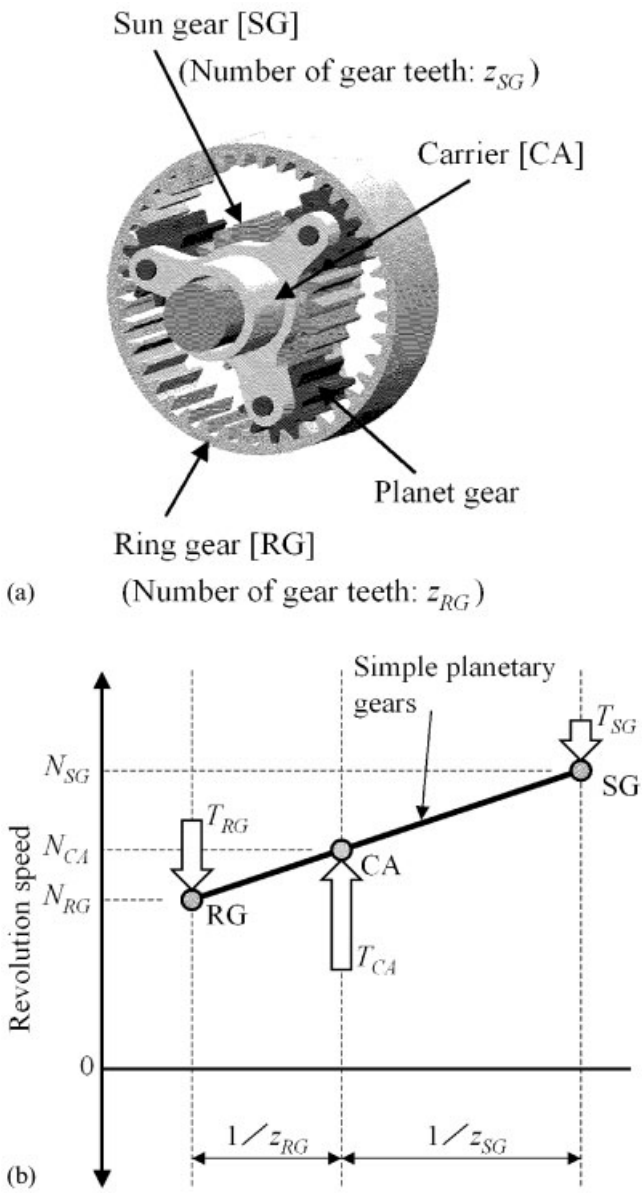

Fig. 2 Simple planetary gears: (a) mechanism; (b) velocity diagram

The diagram is drawn by the following procedure. First, with reference to Fig. 2(a), the rotating direction of the ring gear is confirmed as the reverse of the sun gear when the carrier is fixed. Then the point of the ring gear is placed on the horizontally opposite side of the sun gear from the point of the carrier in the velocity diagram, because of its reverse rotation. The horizontal distances of the ring gear and the sun gear from the carrier are proportional to the inverse of the number of teeth of each element.

According to these rules and with the vertical axis representing the revolution speed, the points of three elements of the simple planetary gears are on the straight line labelled Simple planetary gears in Fig. 2(b). The straight line can move in the vertical direction and change its slope, corresponding to two degrees of freedom of the system.

Denoting the torque of the carrier by T_{CA}, the torque of the sun gear by T_{SG}, and the torque of the ring gear by T_{RG}, these are represented as force arrows in Fig. 2(b). The straight line in the diagram acts as a lever to balance the applied force as well. Therefore, when the forces are balancing and each element is revolving at constant speed, the equations obtained are

$$T_{CA} = T_{SG} + T_{RG} \tag{5}$$

$$T_{SG}\left(\frac{1}{z_{SG}}\right) = T_{RG}\left(\frac{1}{z_{RG}}\right) \tag{6}$$

where z is the number of gear teeth.

From these equations, T_{SG} and T_{RG} are represented by T_{CA} according to

$$T_{SG} = T_{CA}\frac{z_{SG}}{z_{SG} + z_{RG}} \tag{7}$$

$$T_{RG} = T_{CA}\frac{z_{RG}}{z_{SG} + z_{RG}} \tag{8}$$

3.2 Velocity diagram of the active yaw control differential

Figures 3(a) and (b) show the section drawing and schematic diagram of the AYC differential, the world's first production TVD. This mechanism consists of a differential gear unit using bevel gears, a three-cluster

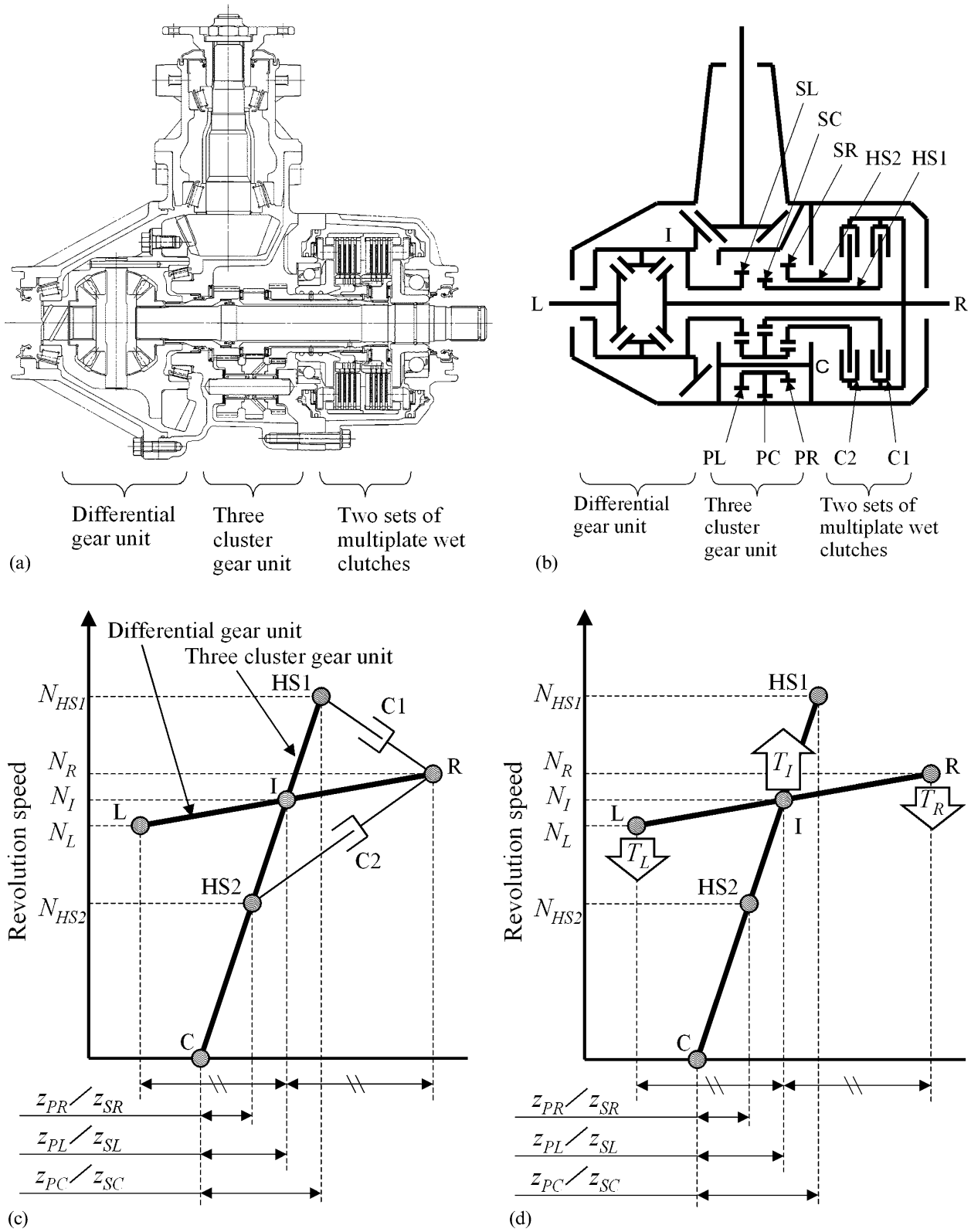

Fig. 3 AYC differential: (a) section drawing; (b) schematic diagram; (c) velocity diagram; (d) torque relation without torque vectoring

gear unit, and two sets of multiplate wet clutches. The differential gear unit is represented by the lever L–R in Fig. 3(c). The left output shaft (L) and the right output shaft (R) are placed at an equal distance from the differential case (I) because the differences in the revolution speed from that of the differential case are the same and the directions are opposite to each other. This figure represents the state where the vehicle is cornering left, and so the revolution speed of point R is faster than that of point L.

The three-cluster gear unit consists of three main gears and a three-gang counter-gear. Each of the three main gears is connected to the differential case I, the first hollow shaft HS1, and the second hollow shaft HS2. Considering the three main gears as three sun gears, and the counter-gear as a planet gear, this unit can be regarded as the planetary gears with the carrier C fixed to housing. With the carrier C fixed, three sun gears revolve as each gear ratio in the same direction, and the left sun gear is connected to the differential case I. This unit is represented by the lever C-HS1 shown in Fig. 3(c), where point C is fixed to the horizontal axis and point I is connected to the lever L–R. The points HS2, I, and HS1 are arranged in the order of the gear ratio from point C. Thus the differential gear unit of three elements with two degrees of freedom and the three-cluster gear unit of three elements with one degree of freedom share one element. Therefore the AYC differential is a mechanism of five elements with two degrees of freedom. The right clutch C1 installed between the first hollow shaft and the right output shaft is drawn between point HS1 and point R, and the left clutch C2 installed between the second hollow shaft and right output shaft is drawn between point HS2 and R, therefore Fig. 3(c) is completed. Figure 3(d) shows the torque when the clutch does not work.

A slipping multiplate wet clutch (called the slip clutch below) transfers torque proportional to the clutch pressure from a faster rotational element to a slower rotational element. Therefore, when C1 is actuated without lock-up, torque is transferred from point HS1 to R so that the right output shaft torque increases. On the other hand, when C2 is actuated without lock-up, torque is transferred from point R to point HS2, so that the right output shaft torque decreases. For a simple explanation, only the function of C1 is explained in detail below.

Consider the case where the torque T_I is supplied to I from the engine, and C1 is actuated without lock-up so that it transfers the torque T_{C1} to point R. T_{C1} acts on point R upwards and, conversely, acts on point HS1 downwards, as shown in Fig. 4. The force balance of lever L–R and the moment balance around point I in Fig. 4(a) give

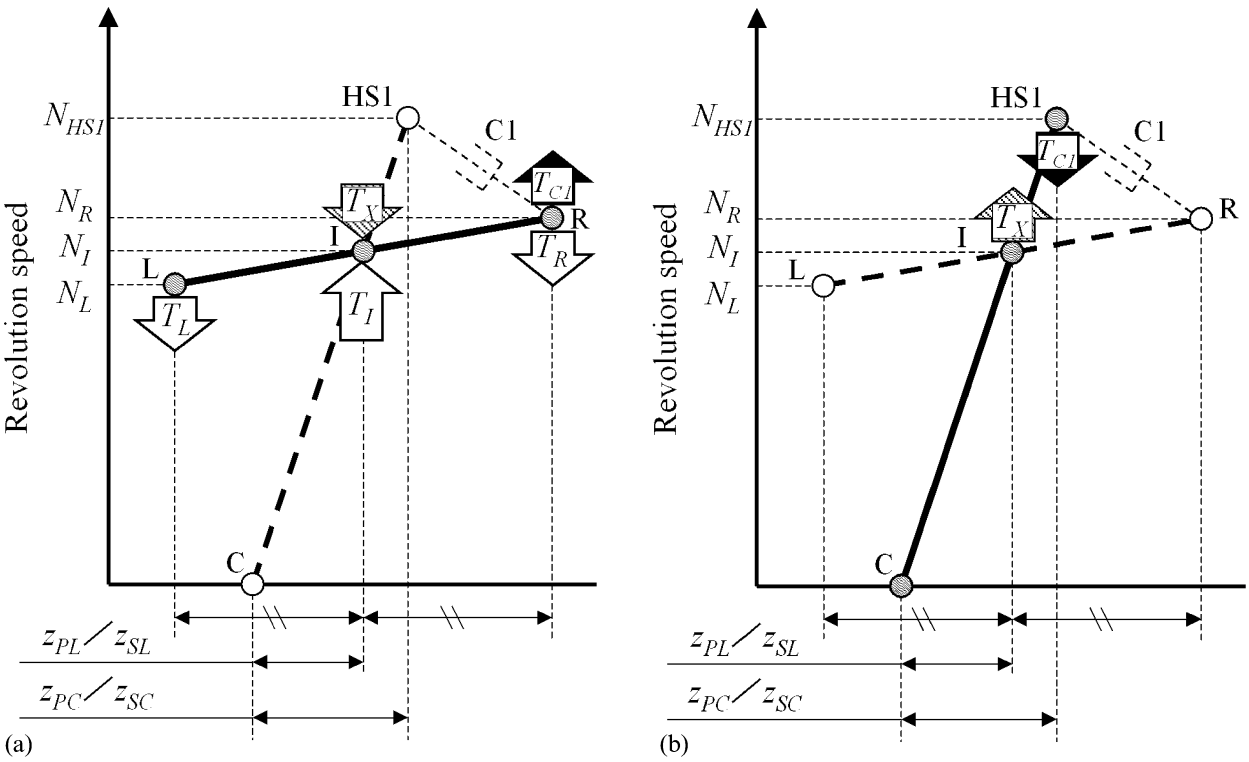

Fig. 4 Right clutch function of the AYC differential: (a) part of differential gear unit; (b) part of three-cluster gear unit

$$T_I + T_{C1} = T_L + T_R + T_X \tag{9}$$

$$T_L = T_R - T_{C1} \tag{10}$$

where T_L is the left output torque, T_R is the right output torque, and T_X is the reaction torque from lever C-HS1. Moreover, since the forces shown in Fig. 4(b) act on the three-cluster gear unit, the moment balance of lever C-HS1 around point C is represented as

$$T_X \frac{z_{PL}}{z_{SL}} = T_{C1} \frac{z_{PC}}{z_{SC}} \tag{11}$$

From equations (9) to (11), the right and left output torques are obtained as

$$T_L = \frac{T_I}{2} - \frac{z_{PC}\, z_{SL}}{2 z_{SC} z_{PL}} T_{C1} \tag{12}$$

$$T_R = \frac{T_I}{2} + \left(1 - \frac{z_{PC}\, z_{SL}}{2 z_{SC} z_{PL}}\right) T_{C1} \tag{13}$$

These expressions clearly show that the slip connection of C1 cause the left output torque to decrease, and the right output torque to increase. The torque difference between the right and left wheels is

$$\Delta T = T_R - T_L = T_{C1} \tag{14}$$

Thus, by using the velocity diagram, it can easily be seen that the AYC differential can generate the torque difference ΔT between the right and left wheels independent of the input torque T_I. This corresponds to the generation of ΔD in Fig. 1.

4 CLUTCH-TYPE LATERAL TORQUE-VECTORING DIFFERENTIALS

4.1 Classification of clutch-type lateral torque-vectoring differentials

Consider a one-way TVD, which transfers torque from the left to the right wheel by using a clutch. The elements related to this TVD are four: L, I, R, and HS1 in Fig. 3. L, I, and R are the necessary three elements of a differential. HS1, which is the speed increase element of I, gives the revolution speed difference of the fixed direction on the slip clutch C1 and makes C1 transfer torque from the left to the right wheel. Thus, the fourth element HS1 is also necessary for one-way TVD. This is a mechanism of four elements with two degrees of freedom, and this is the simplest mechanism composed of the smallest number of rotational elements.

Here, the slip clutch C1 transfers torque from point I to R directly. In this sense, this paper calls I the 'transceiver element' and R the 'receiver element'. The number of variations of one-way TVD represented in the velocity diagram is 12, namely the combinations of three choices of the transceiver element from point L, I, and R, two choices of the receiver element from the remaining, and two choices of the speed of HS1, i.e. increase or decrease. However, since the speed of the left element connected by slip clutch C1 must be faster than that of the right element to transfer torque from the left to the right wheel, the number of variations reduces to the six kinds shown in Table 1 and Fig. 5. Here, TVDs such as IH-O are designated by the following rule. The lettes on the left-hand side of the hyphen represent the torque transceiver element, and those on the right-hand side indicate the receiver element. The symbol I means the input element of differential gear unit shown as point I, and the symbol O means the output of differential gear unit, namely point L or R. The symbol H and L represent increase and decrease respectively in speed.

From this classification, it may be concluded that the AYC differential consists of the IH-O type as the one-way TVD from left to right, and the O-IL type as the one-way TVD from right to left. In the same way, the TVD described in reference [**15**] consists of two I-OL types for both directions, and the TVD described in reference [**16**] consists of the OH-O type as the torque vectoring from left to right, and the O-OL type as the torque vectoring from right to left.

If a TVD of four elements with two degrees of freedom is represented in the schematic figure, many

Table 1 Variation in clutch type TVD

Type	Transceiver element	Receiver element	Speed increase or decrease
IH-O	**I**nput of differential (point I)	Output of differential (point R)	High (speed increase)
OH-I	**O**utput of differential (point L)	Input of differential (point I)	High (speed increase)
OH-O	**O**utput of differential (point L)	Output of differential (point R)	High (speed increase)
O-IL	**O**utput of differential (point L)	Input of differential (point I)	Low (speed decrease)
I-OL	**I**nput of differential (point I)	Output of differential (point R)	Low (speed decrease)
O-OL	**O**utput of differential (point L)	Output of differential (point R)	Low (speed decrease)

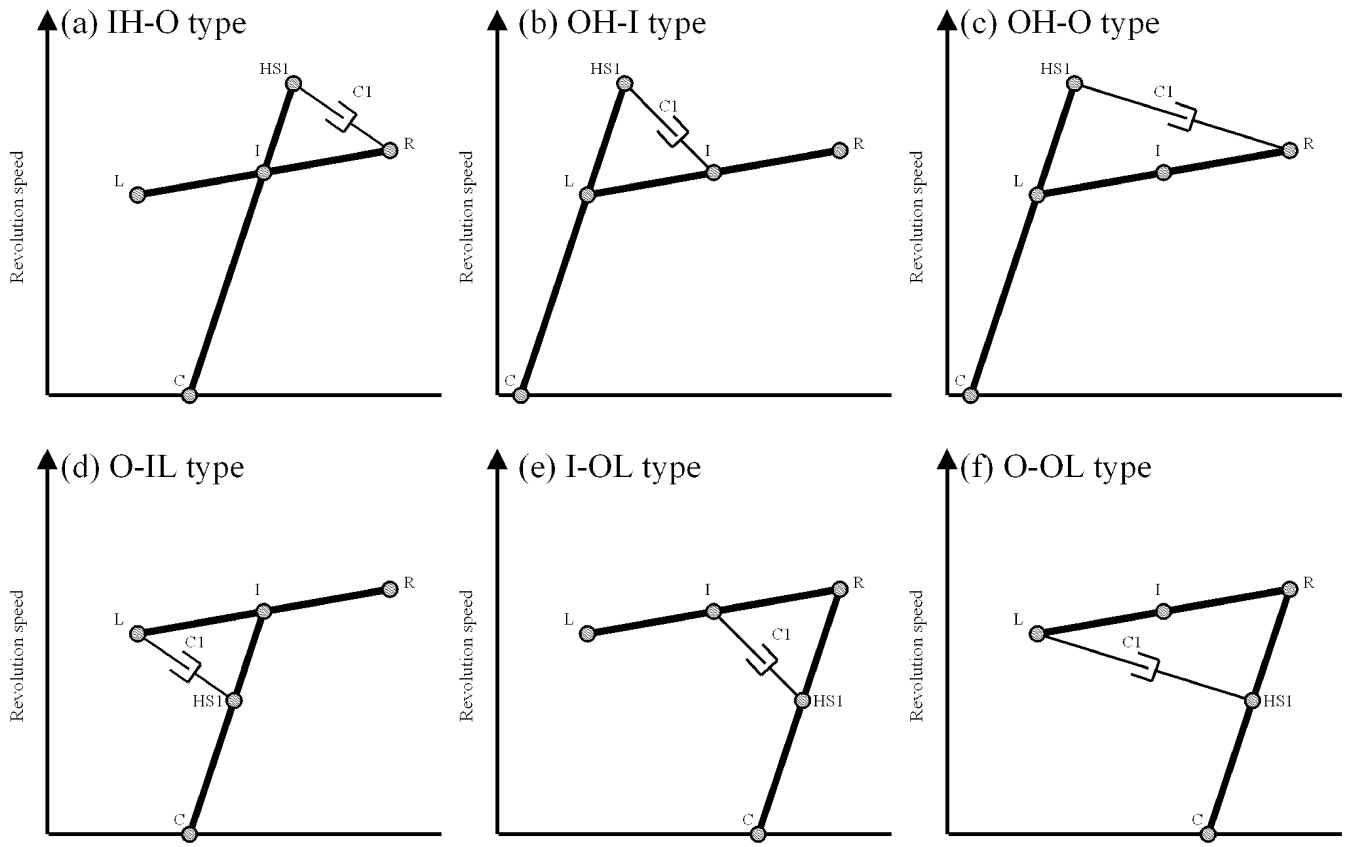

Fig. 5 Variation in the clutch-type TVD

kinds of TVD will be presented. This is due to the variation in the differential mechanisms as well as the mechanism that gives the revolution speed difference of the fixed direction on the slip clutch. On the other hand, once the TVD is represented by the velocity diagram, it turns out that the clutch-type TVD is substantially classified into six kinds. This is the merit and effectiveness of the application of the velocity diagram to the TVD analysis.

4.2 Maximum acceptable differential speed ratio

In order to compare the characteristic of various TVDs on the velocity diagram without considering the actual numbers of the gear teeth of each mechanism, the present authors introduced a new design parameter, namely the maximum acceptable differential speed ratio S_{max}. Figure 6 shows a revolution speed relation of a differential during vehicle cornering, where R is the vehicle's cornering radius, N_L is the left-wheel speed, N_I is the differential case speed, and N_R is the right-wheel speed. The differential speed between the right and left wheels of a cornering vehicle is represented by

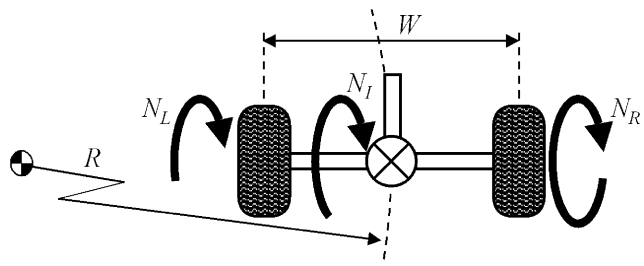

Fig. 6 Speed relation during cornering

$$N_R - N_L = \frac{W}{R} N_I \tag{15}$$

The relation for the differential mechanism is

$$N_I = \frac{N_R + N_L}{2} \tag{16}$$

Eliminating N_L from equation (15) by substituting equation (16) and dividing both sides by N_I gives

$$S = \frac{N_R - N_I}{N_I} = \frac{W}{2R} \tag{17}$$

Here, S is the differential speed ratio between the right wheel and the differential case. Consider the possible differential speed ratio S. Since the vehicle track is constant, equation (17) implies that the differential speed ratio S is inversely proportional to the cornering radius. Thus, a smaller cornering radius causes S to increase. In the case of a compact passenger vehicle, the vehicle track is around 1.5 m, and the minimum cornering radius is around 5 m, so that the possible differential speed ratio is

$$S < 0.15 \tag{18}$$

Here, an IH-O type TVD, which is used for torque vectoring from the left to the right wheels of AYC shown in Fig. 4, is considered as an example. The non-dimensional revolution speeds of each element are defined using equations (16) and (17) as

$$S_{\mathrm{L}} = \frac{N_{\mathrm{L}}}{N_{\mathrm{I}}} = 1 - S \tag{19}$$

$$S_{\mathrm{R}} = \frac{N_{\mathrm{R}}}{N_{\mathrm{I}}} = 1 + S \tag{20}$$

$$S_{\mathrm{HS1}} = \frac{N_{\mathrm{HS1}}}{N_{\mathrm{I}}} \tag{21}$$

The vertical axis of the velocity diagram is represented using these speeds, and Fig. 7(a) is obtained.

Clutch-type TVDs generate the differential speed of the slip clutch by a gear set with a fixed gear ratio. In the case when S_{R} becomes greater than S_{HS1}, the TVD transfers the torque to the opposite direction from that intended. To solve this problem, it is possible to design a gear ratio to make S_{HS1} large. However, in doing this, since the differential speed of slip clutch becomes large when a vehicle drives straight for example, another problem occurs, i.e. the frictional heat of slip clutch become large. Therefore, the minimum cornering radius that the TVD should function at is determined. The differential speed ratio S in this situation, where the revolution speeds of point R and HS1 are equal, shown in Fig. 7(b), is denoted by the maximum acceptable differential speed ratio $S_{\max}$. From equation (20)

$$S_{\mathrm{HS1}} = S_{\mathrm{R}} = 1 + S_{\max} \tag{22}$$

Thus, by using $S_{\max}$ as a design parameter, various TVDs can be represented in the velocity diagram without considering the actual number of gear teeth of the mechanism. From the inequality (18), $S_{\max}$ which is set around 0.1–0.2 is sufficient for a TVD to cover almost all vehicle cornering, so that $S_{\max}$ is assumed to be much smaller than 1 in this paper.

4.3 Characteristics of clutch-type lateral torque-vectoring differentials

By using $S_{\max}$, the IH-O type characteristics, such as the output torque of the right and the left wheels, the

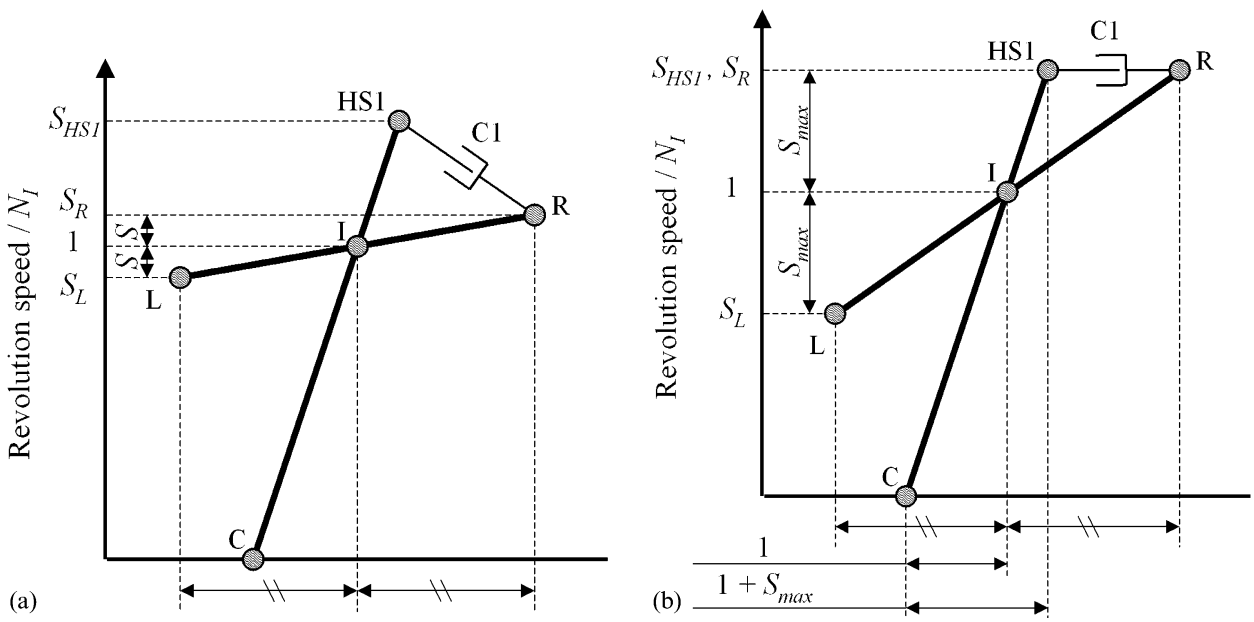

Fig. 7 Velocity diagram of IH-O type: (a) state capable of torque vectoring; (b) state not capable of torque vectoring

clutch torque required to generate the output torque difference, the clutch slip speed, and the energy loss of the mechanism, can be represented.

Figure 8(a) shows a schematic example of an IH-O-type TVD, and Fig. 8(b) shows the dimensionless velocity diagram of the IH-O-type TVD. Figure 8(b) indicates the situation where the input torque T_I acts on the input element I, and the slip clutch C1 transfers the torque T_{C1}. In the figure, the force acting on the lever L–R is represented under the lever L–R, and the force acting on the lever C-HS1 is represented above the lever L–R. As described above equation (22), the revolution speed relation between point HS1 and point I satisfies, from Fig. 8(b)

$$S_{HS1} : 1 = 1 + S_{max} : 1 \tag{23}$$

The force balance on the lever L–R and the moment balance around point I are evidently the same as equations (9) and (10), while the moment balance of the lever C-HS1 around point C is represented by

$$T_X = (1 + S_{max}) T_{C1} \tag{24}$$

From equations (9), (10), and (24), the output torques of the right and left wheels are obtained as

$$T_L = \frac{T_I}{2} - \frac{1 + S_{max}}{2} T_{C1} \tag{25}$$

$$T_R = \frac{T_I}{2} + \frac{1 - S_{max}}{2} T_{C1} \tag{26}$$

From equations (25) and (26), the clutch torque T_{C1} required to generate the output torque difference ΔT ($= T_R - T_L$) between the right and the left wheels is

$$T_{C1} = \Delta T \tag{27}$$

Denoting the differential speed of the slip clutch by ΔS_{C1}, this is the difference between point HS1 and R and is given by

$$\Delta S_{C1} = S_{max} - S \tag{28}$$

The slip clutch generates frictional heat when the clutch transfers the torque. This heat energy is the theoretical energy loss of TVD in the ideal state where neither the transmission efficiency of the gears nor the agitation loss is considered. The energy loss E_{LOSS} is, therefore, evaluated by the product of the clutch torque and the clutch differential speed according to

$$E_{LOSS} = \Delta S_{C1}\ T_{C1} = (S_{max} - S)\ \Delta T \tag{29}$$

The characteristics of the IH-O type TVD are obtained as above.

The other five types of TVD are analysed in the same way. Typical schematic diagrams, the velocity diagrams, and the characteristics of these TVDs are summarized in Table 2. The equations in the table clearly show that all clutch-type TVDs can generate the torque difference ΔT between the right and the left wheels independent of the input torque and that the energy losses E_{LOSS} of all types are completely the same.

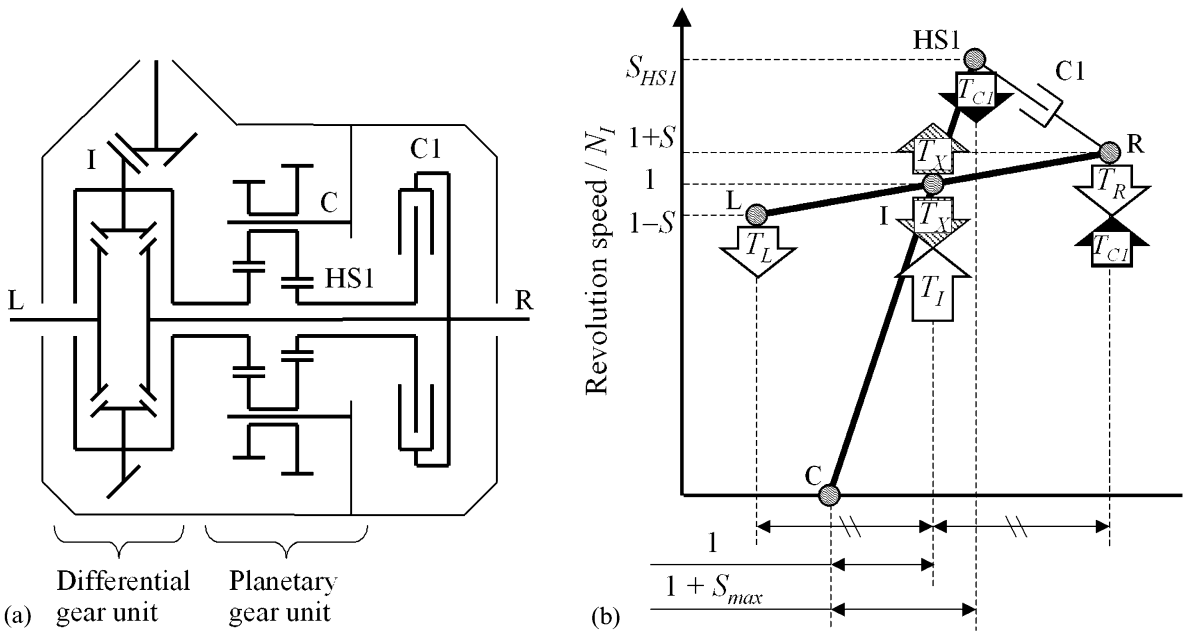

Fig. 8 IH-O type TVD: (a) schematic example; (b) velocity diagram with torque relations

Table 2 Clutch-type TVDs

Type	Typical schematic diagram	Velocity diagram	Equations
OH-I	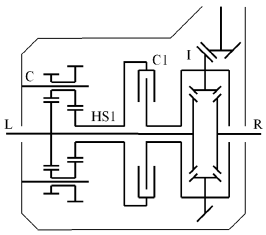	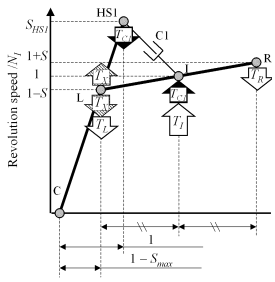	$T_L = \frac{T_I}{2} - \frac{1+S_{max}}{2(1-S_{max})} T_{C1}$ $T_R = \frac{T_I}{2} + \frac{T_{C1}}{2}$ $T_{C1} = (1 - S_{max})\ \Delta T$ $\Delta S_{C1} = \frac{S_{max} - S}{1 - S_{max}}$ $E_{LOSS} = (S_{max} - S)\ \Delta T$
OH-O	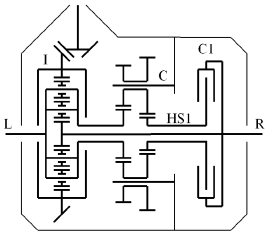	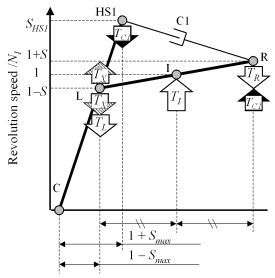	$T_L = \frac{T_I}{2} - \frac{1+S_{max}}{1-S_{max}} T_{C1}$ $T_R = \frac{T_I}{2} + T_{C1}$ $T_{C1} = \frac{1-S_{max}}{2}\ \Delta T$ $\Delta S_{C1} = \frac{2(S_{max} - S)}{1 - S_{max}}$ $E_{LOSS} = (S_{max} - S)\ \Delta T$
O-IL	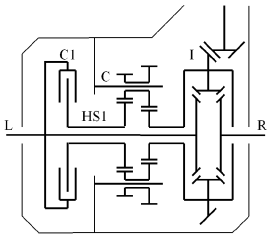	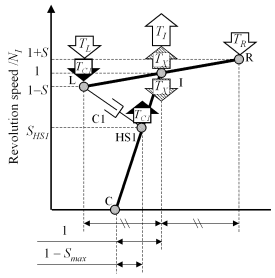	$T_L = \frac{T_I}{2} - \frac{1+S_{max}}{2} T_{C1}$ $T_R = \frac{T_I}{2} + \frac{1-S_{max}}{2} T_{C1}$ $T_{C1} = \Delta T$ $\Delta S_{C1} = S_{max} - S$ $E_{LOSS} = (S_{max} - S)\ \Delta T$
I-OL	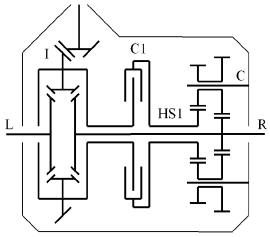	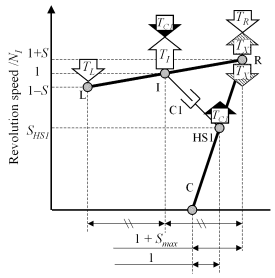	$T_L = \frac{T_I}{2} - \frac{T_{C1}}{2}$ $T_R = \frac{T_I}{2} + \frac{1-S_{max}}{2(1+S_{max})} T_{C1}$ $T_{C1} = (1+S_{max})\ \Delta T$ $\Delta S_{C1} = \frac{S_{max} - S}{1 + S_{max}}$ $E_{LOSS} = (S_{max} - S)\ \Delta T$
O-OL	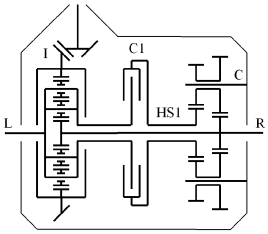	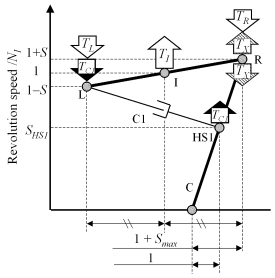	$T_L = \frac{T_I}{2} - T_{C1}$ $T_R = \frac{T_I}{2} + \frac{1-S_{max}}{1+S_{max}} T_{C1}$ $T_{C1} = \frac{1+S_{max}}{2}\ \Delta T$ $\Delta S_{C1} = \frac{2(S_{max} - S)}{1 + S_{max}}$ $E_{LOSS} = (S_{max} - S)\ \Delta T$

5 BRAKE-TYPE LATERAL TORQUE-VECTORING DIFFERENTIALS

5.1 Classification of brake-type lateral torque-vectoring differentials

The brake-type one-way TVD consists of a slip brake and a planetary gear mechanism of four elements with two degrees of freedom. The number of elements and the number of degrees of freedom are the same as those of the clutch-type TVDs. Figure 9(a) shows a schematic example of the brake-type TVD. This is constructed from the schematic diagram of the IH-O-type TVD.

In Fig. 8, when the slip clutch C1 transfers torque and torque vectoring occurs, the reaction torque is applied to the carrier C fixed to the housing. The function of the slip brake in Fig. 9(a) is equivalent to that of the slip clutch in Fig. 8(a). Therefore, the slip brake is labelled C1 in this paper. In the velocity diagram, the differential gear unit is represented as the lever L–R connecting points L, I, and R, and the planetary gear unit is represented as the lever C–R connecting points C, I, and R. These units share the two elements I and R; consequently the brake-type TVD is represented as the lever C–R, which connects points C, L, I, and R with slip brake C1 placed between point C and H, as shown in Fig. 9(b).

Similarly, the brake-type TVDs are constructed from the other schematic diagrams of clutch-type TVDs shown in Table 2. All these TVDs are represented as a lever of four elements with two degrees of freedom and a slip brake in the velocity diagram. Thus, representation of TVDs by the velocity diagram concludes that the brake-type TVDs are classified as only one kind. In fact, the one-way TVDs of various complicated gear mechanisms such as MDT-II described in reference [**12**], the TVD in reference [**13**], and the active torque transfer system in reference [**14**] are represented as a lever shown in Fig. 9(b), although they are proposed as different brake-type TVDs in outward appearance.

5.2 Characteristics of brake-type lateral torque-vectoring differentials

The slip brake C1 is installed between point C and the housing H. Just as clutch-type TVDs, when a smaller cornering radius causes S to increase and the revolution speed of point C to become less than zero, the TVD transfers the torque to the opposite direction that is designed. Therefore, $S_{\max}$ is defined as S when the speed of point C is zero, and the revolution speed relations with point C, L, and I satisfy, from Fig. 9(b)

$$1-S_{\mathrm{C}} : 1-(1-S)=1 : S_{\max} \tag{30}$$

From this, the revolution speed of point C is represented by

$$S_{\mathrm{C}}=\frac{S_{\max}-S}{S_{\max}} \tag{31}$$

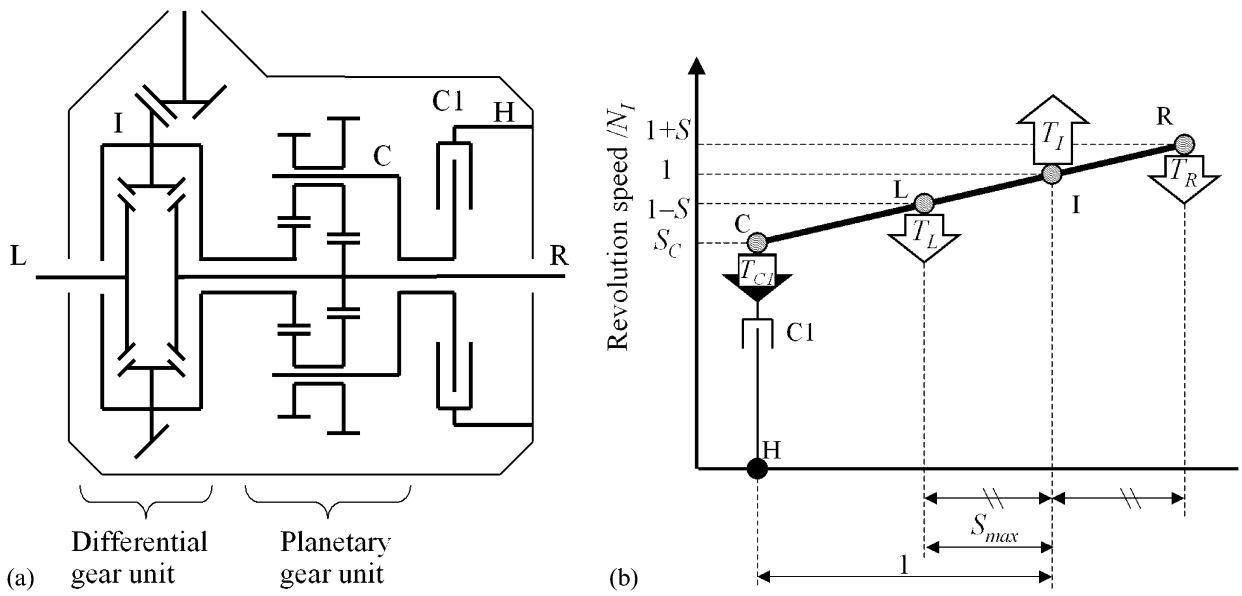

Fig. 9 Brake-type TVD: (a) schematic example; (b) velocity diagram with torque relations

Table 3 Characteristic equations of TVDs

Type	T_{C1}	ΔS_{C1}	E_{LOSS}
IH-O	ΔT	$S_{max} - S$	$(S_{max} - S)\ \Delta T$
OH-I	$(1 - S_{max})\ \Delta T$	$\frac{S_{max}-S}{1-S_{max}}$	$(S_{max} - S)\ \Delta T$
OH-O	$\frac{1-S_{max}}{2}\ \Delta T$	$\frac{2(S_{max}-S)}{1-S_{max}}$	$(S_{max} - S)\ \Delta T$
O-IL	ΔT	$S_{max} - S$	$(S_{max} - S)\ \Delta T$
I-OL	$(1+S_{max})\ \Delta T$	$\frac{S_{max}-S}{1+S_{max}}$	$(S_{max} - S)\ \Delta T$
O-OL	$\frac{1+S_{max}}{2}\ \Delta T$	$\frac{2(S_{max}-S)}{1+S_{max}}$	$(S_{max} - S)\ \Delta T$
Brake	$S_{max}\ \Delta T$	$\frac{S_{max}-S}{S_{max}}$	$(S_{max} - S)\ \Delta T$

The force balance on the lever C–R and the moment balance around point R are represented by

$$T_I = T_R + T_L + T_{C1} \tag{32}$$

$$S_{max}\ T_I = 2S_{max} T_L + (S_{max} + 1) T_{C1} \tag{33}$$

From equations (32) and (33), the brake torque T_{C1} required to generate the output torque difference ΔT between the right and the left wheels is

$$T_{C1} = S_{max}\ \Delta T \tag{34}$$

The differential speed ΔS_{C1} of the slip brake is the same as the revolution speed S_C itself, giving

$$\Delta S_{C1} = \frac{S_{max} - S}{S_{max}} \tag{35}$$

The energy loss is obtained as

$$E_{LOSS} = \Delta S_{C1}\ T_{C1} = (S_{max} - S)\ \Delta T \tag{36}$$

6 COMPARISON OF LATERAL TORQUE-VECTORING DIFFERENTIAL CHARACTERISTICS

The above examination leads to the conclusion that TVD is classified into seven kinds of velocity diagram, namely six clutch types and one brake type. For these seven types of TVD, the values for T_{C1}, ΔS_{C1}, and E_{LOSS} are shown in Table 3.

For a simple case, the situation $S = 0$, where the vehicle runs straight, is considered. Indicating the horizontal axis by T_{C1} and the vertical axis by ΔS_{C1}, the seven kinds of TVD are plotted in Fig. 10(a). They are on a hyperbola of

$$T_{C1}\ \Delta S_{C1} = S_{max}\ \Delta T = \text{constant} \tag{37}$$

and it is equal to E_{LOSS}. This may be because E_{LOSS} is the work required for generating the torque vectoring ΔT from the slower rotational element to the faster rotational element within the maximum acceptable differential speed ratio S_{max}.

Here, the best TVD design is discussed from an actual mechanism design point of view. T_{C1} for the brake-type TVD, the required clutch torque for ΔT, is the smallest, and so this type seems to have the possibility of miniaturization. However, this type needs highly precise parts because the torque vectoring is very sensitive even to a slight clutch torque change, which is frequently influenced by clutch drag for example. In addition, this type has the largest ΔS_{C1}, the differential speed of the slip clutch, and so a countermeasure for clutch drag is needed. In contrast,

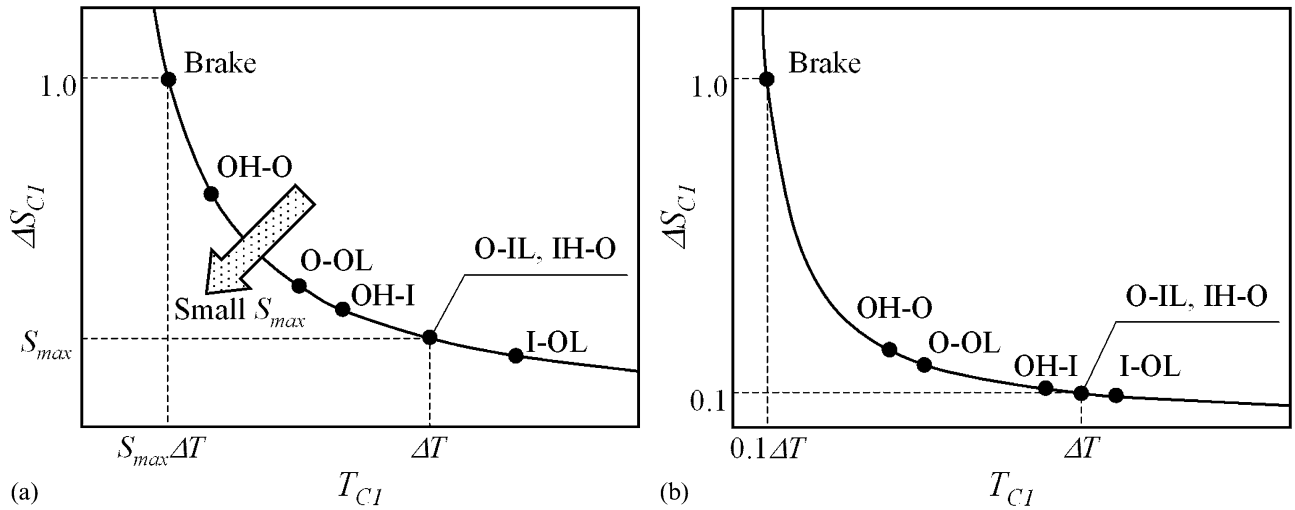

Fig. 10 Relation between T_{C1} and ΔS_{C1}: (a) in the case when $S = 0$; (b) in the case when $S = 0$ and $S_{max} = 0.1$

a clutch-type TVD has small drag. Therefore, this type can improve the clutch response by making the clutch clearance small. Furthermore, the energy losses E_{LOSS} are completely the same for all seven kinds of TVD. Since this energy loss relates to the rise in the temperature of a clutch or brake, the clutch size can be designed to be the same in all seven kinds of TVD from the viewpoint of clutch heat mass. Consequently, it may be concluded that the clutch type is superior as a TVD from the viewpoint of required accuracy, drag loss, and miniaturization. In the case when S_{max} becomes small in Fig. 10(a), the hyperbola will become close to the origin. Figure 10(b) shows the relation between T_{C1} and ΔS_{C1} when S_{max} is set at 0.1. This demonstrates that the OH-O type and the O-OL type are the best choice as a TVD, which reduce both T_{C1} and ΔS_{C1}.

7 CONCLUSION

The structures of TVDs are complicated and it is not very easy to understand their mechanisms and characteristics, although control of the yaw moment is a key to active safe driving and cornering of vehicles. In this paper, an effective use of the velocity diagram was proposed to represent the mechanisms of lateral TVDs and to derive their characteristics such as the required clutch torque for generating the torque difference between the left and the right wheels, the clutch differential speed, and the energy loss. Conclusions may be summarized as follows.

1. The velocity diagram representation is useful for understanding the mechanism of TVDs and classifying them.
2. The simplest one-way TVD is a planetary gear mechanism of four elements with two degrees of freedom.
3. TVDs of four elements with two degrees of freedom are classified into seven kinds in all, namely six clutch types and one brake type.
4. In the case of the ideal state where neither the transmission efficiency of the gears nor the agitation loss is considered, the theoretical values of energy loss are completely the same in these seven kinds of TVD.
5. By using the maximum acceptable differential speed ratio S_{max} as a design parameter, the characteristics of various TVDs can be compared on the velocity diagram without considering the actual numbers of gear teeth of the mechanism.
6. The OH-O type or O-OL type shown in this paper is well balanced to reduce both the required clutch torque and the clutch differential speed, and so these types may be the best selection in actual TVD design.

ACKNOWLEDGEMENT

The authors would like to thank Mr Ushiroda of Mitsubishi Motors Corporation for a helpful discussion during this work.

REFERENCES

1 **Shibahata, Y., Shimada, K.,** and **Tomari, T.** The improvement of vehicle maneuverability by direct yaw moment control. In Proceedings of the First International Symposium on *Advanced vehicle control* (*AVEC '92*), Yokahama, Japan, 14–18 September 1992, 1993, paper 923081, pp. 452–457 (Japan Society of Automotive Engineers, Tokyo); *Vehicle System Dynamics*, 1993, **22**(5), 465–481.

2 **Motoyama, S., Uki, H., Isoda, K.,** and **Yuasa, H.** Effect of traction force distribution control on vehicle dynamics. Proceedings of the First International Symposium on *Advanced vehicle control* (*AVEC '92*), Yokahama, Japan, 14–18 September 1992, paper 923080, pp. 447–451 (Japan Society of Automotive Engineers, Tokyo); *Vehicle System Dynamics*, 1993, **22**(5), 455–464.

3 **Inagaki, S., Kshiro, I.,** and **Yamamoto, M.** Analysis on vehicle stability in critical cornering using phase-plane method. In Proceedings of the Second International Symposium on *Advanced vehicle control* (*AVEC '94*), Tsukuba, Japan, 24–28 October 1994, paper 9438411, pp. 287–292 (Japan Society of Automotive Engineers, Tokyo).

4 **Müller, A., Achenbach, W., Schindler, E., Wohland, T.,** and **Mohno, G.-W.** Das neue Fahrsicherheitssystem electronic stability program von Mercedes-Benz. *ATZ Automobiltechnische Z.*, 1994, **11**, 656–670.

5 **Ikushima, Y.** and **Sawase, K.** A study on the effect of active yaw moment control. SAE paper 950303, 1995.

6 **Sawase, K.** and **Sano, Y.** Application of active yaw control to vehicle dynamics by utilizing driving/braking force. *JSAE Rev.*, 1999, **20**, 289–295.

7 **Sawase, K., Ushiroda, Y.,** and **Inoue, K.** Effect of the right-and-left torque vectoring system in various types of drivetrain. SAE paper 2007-01-3645, 2007.

8 **Andreasson, J., Knobel, C.,** and **Bünte, T.** On road vehicle motion control striving towards synergy. In Proceedings of the Eighth International Symposium on *Advanced vehicle control* (*AVEC '06*), Taipei, Taiwan, 20–24 August 2006, paper 060209, pp. 1–7 (Japan Society of Automotive Engineers, Tokyo).

9 **Schiebahn, M., Zegelaar, P. W. A.,** and **Hofmann, O.** Yaw torque control for vehicle dynamics systems. VDI-Berichte 2014, 2007, pp. 101–119.

10 **He, J., Crolla, D. A., Levesley, M. C.,** and **Manning, W. J.** Integrated chassis control through coordination of active front steering and intelligent torque distribution. In Proceedings of the Seventh International Symposium on *Advanced vehicle control* (*AVEC '04*), Arnhem, The Netherlands, 23–27 August 2004, paper 20044873, pp. 333–339 (Japan Society of Automotive Engineers, Tokyo).

11 **Lück, T., Freimann, R.,** and **Schneider, E.** Driving dynamics and hybrid combined in the torque-vectoring. *VDI-Berichte*, 2007, **2014**, pp. 135–150.

12 **Mohan, S. K., Sharma, A., Mizon, R.,** and **Burns, T.** Torque vectoring systems: architecture, stability performance and efficiency considerations. In Proceedings of the Sixth All-Wheel Drive Congress, Graz, Austria, 2005, pp. 166–180 (Magna Steyr, Graz).

13 **Wheals, J. C.** and **Donin, R.** SUV demonstration of a torque vectoring driveline and new concepts for practical actuation technologies. In Proceedings of the JSAE Annual Congress, 2005, paper 20055433 (Japan Society of Automotive Engineers, Tokyo).

14 **Shibahata, Y., Kuriki, N., Kitamura, K., Honda, K., Wada, K., Kajiwara, H., Nori, A., Kuwahara, K.,** and **Okuma, S.** Development of left–right torque distribution system. *Honda R&D Tech. Rev.*, 1997, **9**, 166–180.

15 **Kober, W.** and **Ramusch, F.** Fahrdynamikbeeinflussung durch kombinierten Einsatz von Hinterachsregelungssystemen. *VDI-Berichte*, 2007, **2014**, pp. 49–64.

16 **Ushiroda, Y., Sawase, K., Takahashi, N., Suzuki, K.,** and **Manabe, K.** Development of super AYC. *Mitsubishi Motors Tech. Rev.*, 2003, **15**, 73–76.

17 **Sawase, K.** and **Inoue, K.** Classification and characteristic analysis of right-and-left torque vectoring mechanisms based on velocity diagram. *VDI-Berichte*, 2007, **2014**, pp. 121–134.

18 **Nagayoshi, Y.** and **Hiramatsu, T.** Dynamic analysis of automatic transmission during gear shifting through velocity diagram on planetary gears. *Mitsubishi Motors Tech. Rev.*, 1989, **1**, 35–40.

19 **Park, J.** and **Kroppe, W.** A study on torque vectoring differential system with 100% torque bias capability. In Proceedings of the Second International Symposium on *Advanced vehicle control* (*AVEC '04*), Arnhem, The Netherlands, 23–27 August 2004, paper 20044860, pp. 251–256 (Japan Society of Automotive Engineers, Tokyo).

20 **Kunii, R., Iwazaki, A., Atsumi, Y.,** and **Mori, A.** Development of SH-AWD (super handling all wheel drive) system. *Honda R&D Tech. Rev.*, 2004, **16**(2), 9–16.

APPENDIX

Notation

D_l	driving force of the left wheel (N)
D_r	driving force of the right wheel (N)
E_{LOSS}	energy loss (W)
M_g	yaw moment acting on the vehicle (N m)
N_{CA}	revolution speed of the carrier (rad/s)
N_{HS1}	revolution speed of the first hollow shaft (rad/s)
N_{HS2}	revolution speed of the second hollow shaft (rad/s)
N_I	revolution speed of the differential case (rad/s)
N_L	revolution speed of the left output shaft (rad/s)
N_R	revolution speed of the right output shaft (rad/s)
N_{RG}	revolution speed of the ring gear (rad/s)
N_{SG}	revolution speed of the sun gear (rad/s)
R	vehicle cornering radius (m)
R_t	radius of the tyre (m)
S	differential speed ratio
S_C	non-dimensional revolution speed of the carrier
S_{HS1}	non-dimensional revolution speed of the first hollow shaft
S_L	non-dimensional revolution speed of the left output shaft
S_{max}	maximum acceptable differential speed ratio
S_R	non-dimensional revolution speed of the right output shaft
T_{CA}	torque of the carrier (N m)
T_{C1}	transfer torque of the slip clutch (N m)
T_e	input torque supplied from the engine (N m)
T_I	input torque of the differential case (N m)
T_L	output torque of the left output shaft (N m)
T_R	output torque of the right output shaft (N m)
T_{RG}	torque of the ring gear (N m)
T_{SG}	torque of the sun gear (N m)
T_V	amount of the vectoring torque (N m)
T_X	reaction torque between the two levers (N m)
W	vehicle track (m)
z_{PC}	number of centre planet gear teeth
z_{PL}	number of left planet gear teeth
z_{PR}	number of right planet gear teeth
z_{RG}	number of ring gear teeth
z_{SC}	number of centre sun gear teeth
z_{SG}	number of sun gear teeth
z_{SL}	number of left sun gear teeth

z_{SR}	number of right sun gear teeth	ΔS_{C1}	non-dimensional differential speed of the slip clutch
ΔD	driving force difference between the right and the left wheels (N)	ΔT	torque difference between the right and the left wheels (N m)